

Nonlinear index of air at 1.053 μm

D. M. Pennington and M. A. Henesian

Lawrence Livermore National Laboratory, P.O. Box 5508, L-493, Livermore, California 94550

R. W. Hellwarth

Department of Electrical Engineering and Department of Physics, University of Southern California, Los Angeles, California 90089-0484

(Received 11 August 1988)

We have measured absolutely the intensity-dependent change in the state of elliptical polarization of a well-characterized 1-ns laser beam propagating in 68 m of air, at intensities ranging from 0.5 to 1.5 GW/cm². From the data we deduce a value for the nonlinear susceptibility coefficient $c_{1221}(-\omega, \omega, \omega, -\omega)$ for air at 20°C and 1.053 μm of $(20 \pm 5) \times 10^{-19}$ esu, corresponding to a nonlinear index $n_2 = 1.0 \times 10^{-16}$ cm³ erg⁻¹. This value is consistent with the value inferred from low-power Kerr and harmonic-generation measurements in O₂ and N₂, but it is approximately one half of a previously reported experimental value for air. We also replaced 58 m of the air path with argon gas at 1 atm pressure and verified that a substantial reduction in nonlinear beam refraction can thereby be achieved.

I. INTRODUCTION

The intensity-dependent change in the state of polarization (ICSP) of a high-power laser beam as it propagates through amplifiers, lenses, and air can cause various effects, such as a reduction in the efficiency of harmonic generation and energy loss from polarizing surfaces. These and other effects of nonlinear refraction, such as self-focusing, of a monochromatic beam in an isotropic transparent medium are described by two medium coefficients, which by common convention are called

$$c_{1111}(-\omega, \omega, \omega, -\omega)$$

and

$$c_{1221}(-\omega, \omega, \omega, -\omega),$$

and referred to as “ c coefficients.”¹ They are also sometimes written as $\chi_{1111}^{(3)}$ and $\chi_{1221}^{(3)}$, although the convention for $\chi^{(3)}$ is not uniform in the literature. (We may omit the frequency arguments of these coefficients as being understood.) The values of these coefficients for common laser and optical glasses have been measured^{2,3} and used in the design of high-power laser chains and target chambers such as the Nova laser system.⁴

Recently, observed reductions from the predicted values of the output at the third-harmonic wavelength from the Nova laser⁴ have been ascribed to the change in polarization of the fundamental beam at 1.053- μm wavelength due to nonlinear propagation in the (~ 65 m) air path between the laser and the harmonic-generating crystals⁵ and to the same effect within the laser amplifier chain itself.⁶ The effect of this nonlinear propagation in isotropic media is mainly to rotate the axes of elliptical polarization of a beam by an angle ψ that is proportional to the product of beam intensity and c_{1221} , as long as ψ is much less than 1 rad.⁷ This ICSP effect is sometimes re-

ferred to as “ellipse rotation.”⁷ We know of only one published c_{1221} c coefficient for air,⁸ and this is a relative measurement which predicts more severe ICSP than we infer from the observed reduction in harmonic-generation efficiency.

To clarify such comparisons and to contribute to future laser design procedures, we have made an absolute measurement of ICSP in air at 1.053- μm wavelength, using a 68-m air path, at 20 ± 1 °C, in the Nova laser beam. The Nova laser is ideally suited to this task because it permits measurements to be performed with an unfocused beam having a uniform spatial profile (described below) and a well-characterized, nearly square, temporal profile. From this measurement, we infer a value for c_{1221} that is about half that reported in Ref. 8. We also replaced 58 m of the 68-m air path with argon gas, at ambient pressure and temperature, and repeated our ICSP measurement. We verified, thereby, that such replacement can be used to reduce ψ by an order of magnitude from its value in air. Our observations on air and argon are consistent with the c coefficients that we have calculated⁹ using published Kerr¹⁰ and harmonic-generation coefficients¹¹ (corrected for dispersion so as to apply at 1.053 μm). The coefficient c_{1221} governing ICSP is ~ 12 times smaller for argon than for air.

In Sec. II we describe the experimental setup for measuring the polarization ellipse rotation angle ψ in three beam configurations, containing (a) air alone, (b) air and two glass windows, and (c) air and argon gas between two glass windows. We also give the data obtained for determining ψ . In Sec. III we describe the procedures we use for assessing the effects of time variations in the optical pulse and the effects of optical misalignment and of uncertainties in the state of the small segment of the Nova beam that we divert for our measurements. To aid in this, we first summarize the standard theory of ellipse rotation. In Sec. IV we use this analysis to interpret our

data and determine the uncertainties in the derived nonlinear coefficient that arise from uncertainties in the characteristics or alignment of detectors, polarizers, the wave plate, and beam splitters. We conclude with a comparison of our results with those of Vlasov *et al.*,⁸ and with the theoretical predictions,⁹ and discuss the potential benefits of substituting argon gas for air in the Nova beam path.

II. EXPERIMENT

In this section we describe the experimental arrangement of optical elements in the 1.053- μm Nova beam path and the data we obtain using this arrangement. We give here only the intended, or "nominal," values of polarizer orientation angles, phase delays, beam diameter and segment lengths, etc. Our estimates of the systematic and statistical deviations from these nominal values will be discussed in Sec. IV.

Our experiments may be described as occurring along a single beam path with polarizers and wave plate oriented as shown in Fig. 1. A well-polarized 25-cm-diam subaperture of one 74-cm-diam Nova beam (delivering from ~ 2 to 6 kJ in 1 ns) was additionally polarized along the (horizontal) reference direction we call \hat{x} (see Fig. 1) by a thin-film Brewster's angle polarizer labeled $P1$ in Fig. 2. This polarizer had a clear aperture of 30 cm and an extinction ratio greater than 200:1. The beam then propagated 15 m past four beam turning mirrors, and sensors (not shown in Fig. 2) which measured the energy and temporal profile of each laser pulse, before impinging on a 10-cm subaperture, AP1 of Fig. 2, placed in the most uniform portion of the beam. Here spatial variations in intensity were generally less than 15%. This subaperture was followed within a few centimeters by a bead-blasted apodizer (to reduce edge diffraction) and a 12-cm-diam crystal-quartz quarter-wave plate (QWP), with its slow axis along a vector \hat{e}_1 oriented at angle $\theta = -26^\circ$. The quarter-wave plate was intended to produce an elliptically polarized beam whose semimajor field component, aligned along \hat{e}_1 , had twice the amplitude of the semiminor component (i.e., ellipticity 0.5). There followed a 68-m propagation path to a diagnostics table

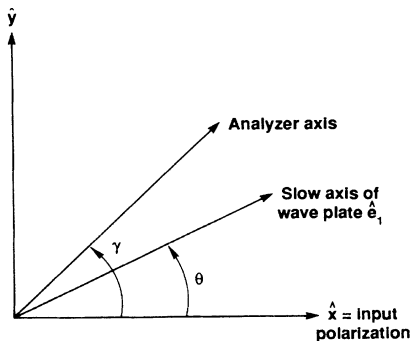


FIG. 1. Definition of axes looking into the beam, i.e., along $-z$.

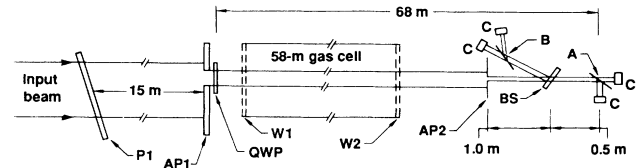


FIG. 2. Experimental arrangement: $P1$ is the input polarizer, AP1 the first (10-cm) aperture and apodizer, QWP is the quarter-wave plate, AP2 is the second (1-in.) aperture, BS is the 50-50 beam splitter that directs beams to the beam-splitting polarizers A and B , whose outputs are monitored by calorimeters C . Three configurations discussed in the text have (a) the 58-m gas cell with its windows $W1$ and $W2$ absent (all air path); (b) the 58-m cell with windows in place and containing air at 1 atm; and (c) the 58-m cell, with windows, containing argon gas at 1 atm.

where the beam encountered a 1-in.-diam aperture AP2 (and a beam splitter BS discussed below) and then propagated 1.5 m to a polarizing beamsplitter A (of the thin-film Brewster type) followed by two calorimeters C , as shown in Fig. 2. These together measured the total beam energy as well as the fraction f_0 of the beam polarized parallel to \hat{x} , the original reference polarization (i.e., at analyzer angle $\gamma = 0$ in Fig. 1). The spatial intensity variations measured after subaperture AP2 were $\sim \pm 1.5\%$. We took the beam area S after this subaperture to be 5.07 cm^2 .

The variation of f_0 with the known beam intensity alone could, in principle, give the desired nonlinear c coefficient. However, because of the anticipated uncertainties in beam parameters a second, independent measurement of polarization was made. This yielded the fraction f_{45} that was polarized at 45° to the original reference polarization \hat{x} . This second measurement was achieved by placing a 50% (nominal) beam splitter BS 0.5 m before polarizer A and oriented so as to direct the split beam at 3° from the backward direction to a polarizing beam splitter B (identical in construction to A). The beam splitter BS in Fig. 2 was 1-cm-thick, 50-mm-diam Schott BK-7 glass flat coated on the front side to reflect 50%, and antireflection coated on the back side. Two calorimeters C monitored the output beams from the polarizing beam splitter B to give the energies polarized at both $\gamma = 45^\circ$ and 135° , thus allowing f_{45} to be deduced independently. We refer to the measurements at B as the "45-135 channel," and the measurements at A as the "0-90 channel." We will call f_γ the fraction passed by a polarizer oriented at angle γ .

Our data will yield a plot of the polarized fractions f_0 and f_{45} of each propagated Nova pulse as a function of an average incident pulse intensity I (to be defined below). In assessing the polarized fractions and their estimated uncertainties, we have taken into account the fact that the polarizing beam splitters erroneously deflect 1.15% of the transmitted polarization (at $\gamma = 0^\circ$ or 135°) into the split beam. Their internal losses are less than 0.5% and were neglected. The four calorimeters were calibrated to an absolute accuracy of $\pm 2.5\%$ and a relative accuracy of

$\pm 1.5\%$. The beam splitter was found to reflect 51% and transmit 48% of the incident light, rotating linearly polarized light by $\sim 2.8^\circ$ (from y to x) upon reflection and $\sim 1.8^\circ$ (from x to y) upon transmission.

The pulse energy U of the 1-in.-diam portion of the beam being analyzed was deduced from the calorimeter readings at both A and B and the parameters mentioned above. The two values of U obtained agreed to within 4%, and their average was used. The values ranged from ~ 2 to 7 J.

Three experimental configurations were used which we will label (a), (b), and (c). These refer to the cases (a) where the 58-m gas cell of Fig. 2 is absent, (b) the 58-m

cell is present, with windows $W1$ and $W2$, containing air, and (c) the 58-m cell is present with argon gas between $W1$ and $W2$.

The temporal pulse shape was nominally a square pulse of 1-ns duration. The actual temporal shape was monitored for each pulse by a streak camera between the initial polarizer and the quarter-wave plate. The effective beam intensity I for ellipse rotation was evaluated for each pulse by the relation

$$I = U / \tau S . \quad (1)$$

The effective pulse length τ was calculated from the unnormalized temporal trace $p(t)$ of the pulse power by the

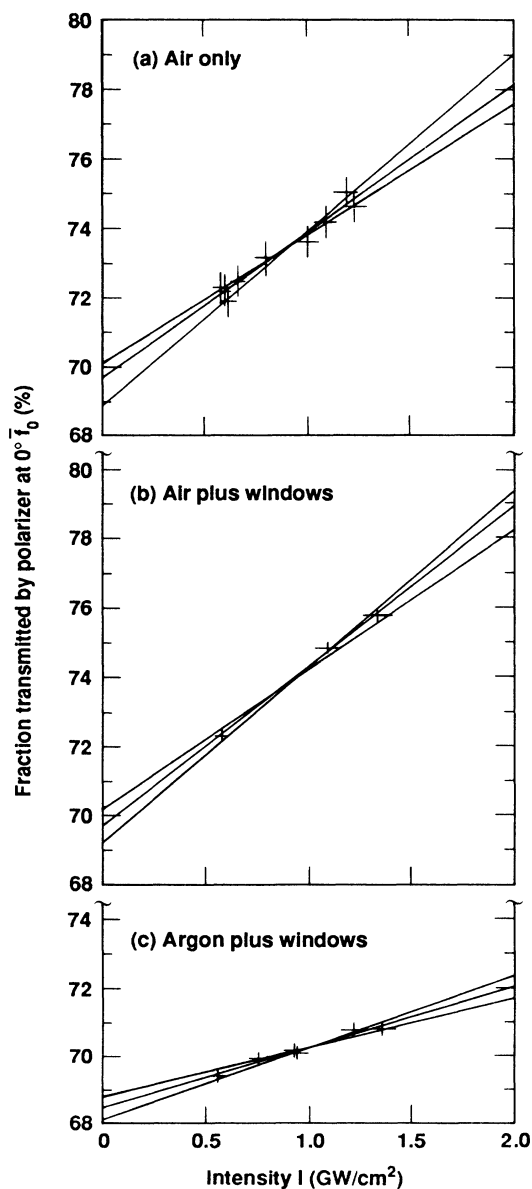


FIG. 3. Transmission \bar{f}_0 through polarizer A as a function of optical intensity; polarizer set parallel to axis of incident polarization. Ordinate is defined in Eq. (3).

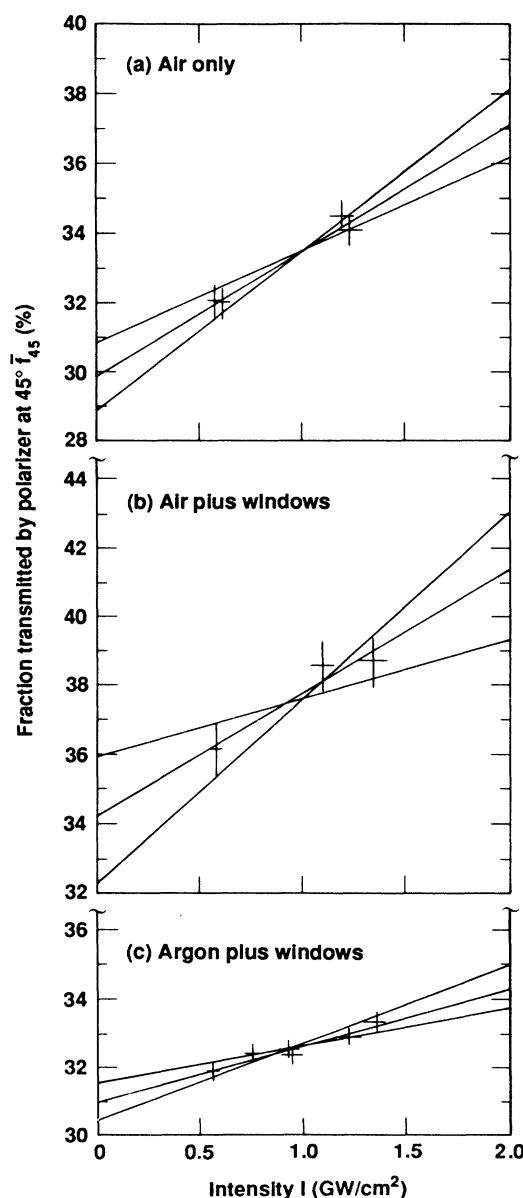


FIG. 4. Transmission \bar{f}_{45} through polarizer B as a function of optical intensity; polarizer axis set at 45° to axis of incident polarization. Ordinate is defined in Eq. (4).

TABLE I. Observed changes in elliptical beam polarization versus beam intensity are represented here by the slopes f'_γ of the data given in Figs. 3 and 4 for two values of analyzing polarizer orientation angle γ . As a result of the corrections of Eqs. (3) and (4), these slopes correspond to the slopes at zero intensity. Also given are the intercepts $f_{\gamma 0}$, which reflect the state of the unchanged (low-intensity) beam polarization. Nominal values were obtained by linear regression analysis. Uncertainties given are derived from the extreme-consistency lines shown in Figs. 3 and 4.

Configuration	$10^4 f'_\gamma$ (cm ² /GW)		$10^3 f_{\gamma 0}$	
	$\gamma=0^\circ$	$\gamma=45^\circ$	$\gamma=0^\circ$	$\gamma=45^\circ$
(a) Air	435±93	391±100	696±8	298±10
(b) Air+windows	480±55	394±180	696±5	340±20
(c) Air+windows+Ar	179±30	168±60	685±4	309±6

following relation, which we justify in Sec. III:

$$\tau = \left[\int dt p(t) \right]^2 / \int dt p^2(t). \quad (2)$$

Because of deviations from the intended square pulse shape, the values of τ thus obtained ranged from 0% to 20% larger than the actual pulse full width at half maximum.

A final small correction was made to the measured polarization fractions f_0 and f_{45} before plotting them against I . The desired nonlinear susceptibility coefficient c_{1221} is proportional to the slope of this plot at small I . In some cases the intensities used were large enough to cause observable (< 10%) deviations from the linearity of f_γ versus I . We used the theory of ellipse rotation given in Sec. III to calculate how f_0 and f_{45} deviate from linearity as I increases. In this calculation we used the known value of the nonlinear indices of the glass windows $W1$ and $W2$ [given after Eq. (17)], and the values for air [see Eq. (19)] and argon [see Eq. (20)] derived⁹ from recent Kerr¹⁰ and second-harmonic¹¹ data. The resulting, slightly modified, polarization fractions \bar{f}_0 and \bar{f}_{45} should be linear functions of intensity I , in the range of our observations, and should have slopes equal to the desired slope f'_γ of the raw data evaluated in the limit of low intensity. These modified fractions are given by

$$\bar{f}_0 \equiv f_0 + \begin{cases} \text{(a) 5.69} \\ \text{(b) 7.48} \\ \text{(c) 0.75} \end{cases} \times 10^{-3} [I(\text{GW cm}^{-2})]^2 \quad (3)$$

and

$$\bar{f}_{45} \equiv f_{45} - \begin{cases} \text{(a) 7.56} \\ \text{(b) 9.93} \\ \text{(c) 1.00} \end{cases} \times 10^{-3} [I(\text{GW cm}^{-2})]^2 \quad (4)$$

where (a), (b), and (c) refer to the three configurations described above.

We give our experimental results for \bar{f}_0 versus I in Fig. 3, and those for \bar{f}_{45} versus I in Fig. 4. The pertinent slopes $f'_\gamma \equiv (\partial \bar{f}_\gamma / \partial I)$ derived from these plots by a linear regression program are given in Table I. Included also are the data intercepts $f_{\gamma 0}$, which represent extrapolated

values for the expected beam polarizations as the intensity approaches zero. Statistical error bars that corresponded to two standard deviations in \bar{f}_γ and $\pm 5\%$ uncertainty in I were assigned to data points. Then the straight lines seen in Figs. 3 and 4 were drawn to fit the extremes allowed by these error bars. The errors quoted in Table I correspond to these extremes. We now develop the theory for relating these results to the derived nonlinear indices.

III. ANALYSIS OF EXPERIMENT

In analyzing the signals from the two polarizers in the observation channels A and B , we will neglect the spatial intensity variations (less than 5%) in the propagated beam and write the optical electric field in the beam as

$$\mathcal{E}(z, t) = \text{Re}[\hat{\mathbf{e}}(z)E(z, t)e^{-i\omega t}], \quad (5)$$

where z is the distance along the beam path and $\hat{\mathbf{e}}$ is the complex polarization vector normalized so that $\hat{\mathbf{e}}^* \cdot \hat{\mathbf{e}} = 1$. The pulse envelope function $E(z, t)$ is assumed to vary negligibly during the linear and nonlinear dielectric response times of the various media (air, windows, etc.). We have experimental indications that the originally x -polarized beam becomes slightly elliptically polarized and slightly tilted in the 15 m before it reaches the quarter-wave plate. Therefore we assume the state of polarization before the quarter-wave plate to be

$$\hat{\mathbf{e}} = \hat{\mathbf{x}} \cos \nu + i \hat{\mathbf{y}} \sin \nu, \quad (6)$$

where $\hat{\mathbf{x}}$ and $\hat{\mathbf{y}}$ are the orthonormal coordinate vectors of Fig. 1. We expect small ellipticity so that $|\nu| \ll 1$. We call the angle of the slow axis of the quarter-wave plate θ as measured from $\hat{\mathbf{x}}$ toward $\hat{\mathbf{y}}$. (By design $\theta \approx -26^\circ$.) The optical phase retardation of the slow axis we call ϕ . A standard polarizer test determined that ϕ was either -87° or -93° with 1° of uncertainty.

Suppose we write the beam polarization as it travels through an isotropic transparent nonlinear medium as

$$\hat{\mathbf{e}}(z) = c_+(z)\hat{\mathbf{e}}_+ + c_-(z)\hat{\mathbf{e}}_-, \quad (7)$$

where

$$\hat{\mathbf{e}}_+ \equiv (\hat{\mathbf{x}} + i\hat{\mathbf{y}})/\sqrt{2} \quad (8)$$

is the normalized vector representing right-circular polarization (from $\hat{\mathbf{x}}$ toward $\hat{\mathbf{y}}$), and $\hat{\mathbf{e}}_- \equiv \hat{\mathbf{e}}_+^*$ is the vector

representing left-circular polarization. Maker *et al.*⁷ showed that the nonlinear optical susceptibility causes the initial amplitude of the right-circular component $c_+(0)$ to be multiplied by a phase $e^{2i\psi(z)}$ relative to the phase of the left-circular component $c_-(z)$. If the i th spatial component of nonlinear polarization density at frequency ω is written as $\text{Re}P_i^{\text{NL}}e^{-i\omega t}$, and its relation to the optical amplitude E_j [the j th spatial component of $\hat{\mathbf{e}}E$ in (5)] is written¹

$$P_i^{\text{NL}} = \sum_{j,k,l=x,y,z} 3c_{ijkl}(-\omega, \omega, \omega, -\omega) E_j E_k E_l^*, \quad (9)$$

then, in isotropic media whose nonlinear response is nearly instantaneous,

$$F_\gamma = \frac{1}{2} + \frac{1}{2} \{ \cos(2\nu) [\cos(2\gamma + 2\psi - 4\theta) \sin^2(\phi/2) + \cos(2\gamma + 2\psi) \cos^2(\phi/2)] + \sin(2\nu) \sin(2\gamma + 2\psi - 2\theta) \sin\phi \}. \quad (11)$$

To compare the predictions of this equation with the experimental results of Figs. 3 and 4, we see that we need only to evaluate (1) the intercept $F_{\gamma 0} \equiv F_\gamma(\psi=0)$, and (2) the slope $F'_\gamma = (\partial F_\gamma / \partial \psi)_{\psi=0}$ with respect to ψ , in order to predict the slope and intercept of the observed fractions f_γ plotted versus intensity. The energy U_γ emerging from a polarizer oriented at γ , and situated at $z=L$ after an interaction path length L , is the time integral of the transmitted power. For small $\psi(L, t)$ this is

$$U_\gamma = \int dt p(t) [F_{\gamma 0} + F'_\gamma \psi(t)], \quad (12)$$

where $p(t)$ is the pulse power incident on the polarizer. Since $\psi(L, t)$ is itself proportional to $p(t)$, we see from (12) that the fraction $f_\gamma \equiv U_\gamma / U$ of energy transmitted by a polarizer at angle γ may be written

$$f_\gamma = F_{\gamma 0} + m_\gamma I, \quad (13)$$

where the average intensity I is defined in (1) and (2). From (10) and (12), we have

$$m_\gamma \equiv -F'_{\gamma 0} (48\pi^2 \omega c_{1221} L / n^2 c^2) M_e, \quad (14)$$

in which

$$M_e \equiv |c_+|^2 - |c_-|^2 \\ = \cos(2\nu) \sin\phi \sin(2\theta) + \sin(2\nu) \cos\phi \quad (15)$$

is the previously mentioned measure of ellipticity that is unchanged by the nonlinear propagation. At this point it is easy to see how, by keeping the next term ($\propto \psi^2$) in the expansion (12), we would obtain the I^2 term from which we calculated the corrections of (3) and (4).

From Eq. (13) we see that we may identify m_γ with the f'_γ we have measured and listed in Table I, and $F_{\gamma 0}$ with the measured intercepts $f_{\gamma 0}$. When there are several materials (labeled by i) of lengths L_i and refractive indices n_i in the propagation path, then the nonlinear coefficients $c_{1221}^{(i)}$ and their uncertainties $\Delta c_{1221}^{(i)}$ must be related to the measured f'_γ and their uncertainties $\Delta f'_\gamma$ (see Table I) by

$$\psi(z, t) = (-6\pi\omega c_{1221} z / nc) (|c_+|^2 - |c_-|^2) |E(z, t)|^2. \quad (10)$$

That is, at (z, t) the pulse has the axes of its polarization ellipse rotated by an angle ψ (in the sense of $\hat{\mathbf{x}}$ to $\hat{\mathbf{y}}$ for $\psi > 0$) that is proportional to the intensity at (z, t) , and to a measure $|c_+|^2 - |c_-|^2$ of the ellipticity that is not changed by nonlinear (or linear) propagation. We omit here, and henceforth, the frequency arguments of the nonlinear susceptibility functions c_{1221} , of which the subscripts 1 and 2 represent any two orthogonal directions. The linear refractive index of the medium is n .

The fraction $F_\gamma(\psi)$ of the above beam that will pass through an ideal linear polarizer oriented at angle γ (from $\hat{\mathbf{x}}$ toward $\hat{\mathbf{y}}$) after the rotation of its polarization ellipse by ψ is

$$\sum_i [c_{1221}^{(i)} \pm \Delta c_{1221}^{(i)}] L_i n_i^{-2} \\ = (c^2 / 48\pi^2 \omega) (f'_\gamma \pm \Delta f'_\gamma) (H_\gamma \pm \Delta H_\gamma), \quad (16)$$

where

$$H_\gamma(\theta, \phi, \nu) \equiv -(F'_{\gamma 0} M_e)^{-1} \quad (17)$$

and where the uncertainty ΔH_γ represents the sum of uncertainties in Eq. (17) arising from uncertainties in the angles γ , θ , ϕ , and ν .

The nominal values of (1) the ellipticity angle ν of the initial polarization state, (2) the orientation θ of the first wave-plate axis $\hat{\mathbf{e}}_1$, (3) the relative retardation $\phi = \phi_1 - \phi_2$ of the optical phase ϕ_2 along the second wave-plate axis with respect to the optical phase ϕ_1 along the first axis, and (4) the angle γ of the axis of the analyzing polarizers (as depicted in Fig. 1) were 0, -26 , -90 , and 0° or 45° respectively. For these values substitution of Eqs. (11) and (15) in Eq. (17) gives $H_0 = 2.616$ and $H_{45} = 3.348$, respectively.

In the three experimental configurations (a), (b), and (c), the sum in Eq. (16) will be assumed to comprise a 68 m of air only, (b) 68 m of air plus windows, and (c) 58 m of argon, and 10 m of air plus windows. We will assume that the BK-7 glass windows have $c_{1221} = 1.8 \times 10^{-15}$ esu,

TABLE II. Values of the nonlinear propagation coefficient c_{1221} , with uncertainties derived from Table I by Eq. (16) with $\Delta H_\gamma = 0$. The experimental configurations (a), (b), and (c) are as in Table I and explained in text. Results are given for two values of analyzing polarizer angle γ .

Configuration	$10^{19} c_{1221}(-\omega, \omega, \omega, -\omega)$ (esu)		
	Material	$\gamma = 0^\circ$	$\gamma = 45^\circ$
(a)	Air	17 ± 4	19 ± 6
(b)	Air	19 ± 3^a	19 ± 9^a
(c)	Argon	$3 \pm 2^{a,b}$	$3 \pm 6^{a,b}$

^aAssumed value for BK-7 windows as given in text.

^bAssumed value for air as given in Eq. (19).

$n=1.51$, and $L=3$ cm, with $\Delta c_{1221}=0.2$.³ Using Eq. (16) we obtain the values given in Table II. Here ΔH_γ was assumed to be zero; the stated errors reflect only the higher and lower sloped lines, drawn to reflect the extremes of consistency with the data points in Figs. 3 and 4. We proceed next to discuss the actual uncertainty ΔH_γ in the parameter H_γ in Eq. (16), which relates the fraction f_γ of the propagated beam passing through a linear polarizer at angle γ to the desired coefficients $c_{1221}^{(i)}$, which predict the state of polarization after nonlinear propagation.

IV. INTERPRETATION AND CONCLUSIONS

We did not appreciate during the Nova experiments how sensitive our final conclusions might be to small deviations (from the intended, or nominal values) of such experimental parameters as the angles ν , θ , ϕ , and γ . Therefore we first discuss here the magnitudes of this sensitivity before concluding what our most probable value for c_{1221} , and its uncertainty, is. If, as we suspect, the values of ν , θ , ϕ , and γ deviate from the nominal values given in the description of the apparatus, and recapitulated after Eq. (17), then we expect both the intercepts and slopes seen in Figs. 3 and 4 to be affected. The nominal values used in Eq. (11) with $\psi=0$ predict, for the low-intensity intercepts (i.e., the polarization fractions), $F_0=0.6895$ and $F_{45}=0.2574$. These are at variance with the ranges closed by the limiting straight lines drawn in Figs. 3 and 4 to reflect our estimate of the uncertainties in the inferred slopes and intercepts imposed by the scatter and uncertainties in the data points. (The deviation is much larger for the 45-135 channel measurements.) Because of the obvious variations among data between configurations (a), (b), and (c), we assume that the windows caused some small but measurable, and different, effect on beam polarization in each experimental configuration. We have not modeled window birefringence in Eq. (11). However, we have independent evidence, obtained after the Nova experiments, on devia-

tions of the four angle parameters whose effects are included in Eq. (11). The extinction ratio of the wave plate between polarizers and other checks showed that the optical retardation angle ϕ was more likely to be $-93^\circ \pm 1^\circ$ than -87° . The beam splitter was observed to cause an effective change in γ by $\sim -2.8^\circ$ in the 45-135 channel and $\sim 1.8^\circ$ in the 0-90 channel, as described previously. Calibration shots with the quarter-wave plate removed gave results suggesting that the original polarization axis was tilted so as to decrease each γ by approximately 1.2° . Calibration shots with the quarter-wave plate rotated to nominal $\theta=0^\circ$ were consistent with an actual $\theta=-26.5^\circ$ (0.5° less than nominal). Both results were also consistent with an ellipticity angle $\nu=-3^\circ$ rather than zero for the polarization incident on the wave plate. By inserting all these angle deviations in Eqs. (11) and (17), and calculating the corrections to predicted intercepts $F_{0\gamma}$ and slope constants H_γ to first order in these changes, we have obtained our best estimates for the corrections $\Delta F_{0\gamma}$ and ΔH_γ , and given them in Table III. These corrections lessen the difference overall between predicted and observed intercepts $F_{\gamma 0}$. However, these corrections are estimates and do not include many other possible corrections that might arise from window birefringence, nonlinear response of polarizers, etc. The effects of any other set of supposed small deviations in ν , ϕ , θ , and γ can be obtained from those given in Table III by linear scaling. The corrections, and their totals, as given in Table III, probably indicate the order of magnitude of the uncertainties introduced by ΔH_γ in Eq. (16).

To proceed to a "best" value for the c_{1221} coefficient of air from our data, we alter the four values for this coefficient given in Table II by the percentages implied by the totals for ΔH_γ in Table III ($+9.3\%$ for 0-90 results, $+6.5\%$ for 45-135 results); we then average these corrected four values, weighted inversely as the percentage errors shown in Table II. This gives, for air at $1.053 \mu\text{m}$ and 20°C ,

TABLE III. Corrections $\Delta F_{\gamma 0}$ to predicted low-intensity polarization fractions $f_{\gamma 0}$, and ΔH_γ to predicted slope factor of Eq. (16). These were derived by computing the first-order variations of the predicted fraction in Eq. (11) with respect to the wave-plate orientation θ , the wave-plate retardation angle ϕ , the analyzing polarizer orientations γ , and the ellipticity angle ν of the incident radiation. The variations used here are explained in the text, as are the nominal values about which variations are taken.

Angle errors (deg)	$10^3 \Delta F_{\gamma 0}$	$10^3 \Delta H_\gamma$ (GW/cm ²)
		$\gamma = 0^\circ$
$\Delta\theta = -0.5$	-8.5	-13
$\Delta\phi = -3$	-16	-137
$\Delta\gamma = 0.65$	-5.5	46
$\Delta\nu = -3$	41	348
Totals	11(+1.6%)	244(+9.3%)
		$\gamma = 45^\circ$
$\Delta\theta = -0.5$	2	-104
$\Delta\phi = -3$	-12	450
$\Delta\gamma = -4$	24	600
$\Delta\nu = -3$	32	-729
Totals	46(+18%)	217(+6.5%)

$$c_{1221}(-\omega, \omega, \omega, -\omega) = (20 \pm 5) \times 10^{-19} \text{ esu} . \quad (18)$$

The uncertainty quoted here is the smallest statistical uncertainty listed in Table II ($\pm 16\%$) increased by $\pm 9\%$ to account for possible systematic errors of a magnitude indicated by Table III. These numbers represent our best estimate of the uncertainties expressed by $\Delta f'_\gamma$ and ΔH_γ , respectively, of Eq. (16). However, we have found with the aid of Table III that other consistent scenarios (e.g., $\Delta\phi = +3$ instead of -3) give c_{1221} values within the limits quoted in (18).

The result (18) agrees well with the value calculated for the same coefficient by some elaborate manipulation of data from both Kerr constant and second-harmonic measurements in N_2 and O_2 (Ref. 9):

$$(23 \pm 2) \times 10^{-19} \text{ esu} . \quad (19)$$

This value includes small dispersion corrections to account for the various measurements having been made at different wavelengths. It is this value that was used in making the small data adjustments described in Eqs. (3) and (4).

It is interesting to note that the cw Kerr measurements¹⁰ and cw harmonic-generation data¹¹ on N_2 and O_2 gases show that c_{1221} of air arises 92% from molecular reorientation, and only 8% from the nonlinear electronic response that would occur if the nuclei were not free to reorient themselves in the optical field.⁹ Although the response time of this reorientation has never been measured, it is likely to be of the order of the inverse of the linewidths (full width at half maximum in rad/sec) seen in rotational Raman scattering. At 1 atm these linewidths are heavily collisional and are of the order of 2×10^{10} radians/sec (3 GHz) for rotational transitions in N_2 .¹² We might expect therefore that our measurements made with 1-ns pulses would show a c_{1221} for air of the order of 5% lower [$10^9 / (2 \times 10^{10})$] than the steady-state value calculated in Eq. (19). This correction appears to be of marginal significance.

To help connect our convention for coefficients with others commonly used, we note that cw Kerr and harmonic-generation data imply $c_{1111} = (3.0 \pm 0.3) \times 10^{-18}$ esu for air at 1.053 μm and 20°C.⁹ This coefficient is often expressed in terms of a nonlinear index n_2 , in terms of which the self-induced change in refractive index experienced by a linearly polarized beam

equals $n_2 \langle \mathcal{E}^2 \rangle$. Then n_2 equals $12\pi c_{1111} / n$. Therefore n_2 for air at 1.053 μm and 20°C equals $(1.1 \pm 0.1) \times 10^{-16}$ esu. This is two orders of magnitude smaller than the values for BK-7 and typical laser glass.

The results given in Tables I and II with argon gas in 58 m of the propagation path give a very uncertain estimate for c_{1221} or argon. Nevertheless, these results confirm that replacing the air in a beam path with argon gas can reduce the polarization ellipse rotation considerably. The value for $c_{1221}(-\omega, \omega, \omega, -\omega)$ of argon gas at 1.053 μm , as calculated from recent Kerr and second-harmonic measurements, is⁹

$$(2.0 \pm 0.1) \times 10^{-19} \text{ esu} , \quad (20)$$

one order of magnitude smaller than the value for air, and quite consistent with the results of our experiments.

Our value (18) of c_{1221} value for air is about half of the most recently published value, 46×10^{-19} esu, deduced by Vlasov *et al.*,⁸ from measurements of intensity-induced polarization changes at 1.06 μm in air, relative to a particular Soviet laser glass (LGS-27). Because this glass is unavailable to us, and because Ref. 8 contains insufficient detail about their unusual "five-focus" beam geometry and diagnostics, we will not speculate on this large discrepancy. We believe, on the bases of our observations, that the best values of c_{1221} to use in beam path calculations for air and argon are those, given in (19) and (20), which are calculated from low-intensity measurements of Kerr effect and optical harmonic generation by the theory of Ref. 9. Our experimental value (18) is consistent with (19). We have also shown that replacing air by argon may be effective in eliminating troublesome nonlinear propagation effects.

ACKNOWLEDGMENTS

We thank C. D. Swift for technical assistance and participation in the experiments, and D. R. Speck for many helpful discussions. The work of D.M.P. and M.A.H. was performed under the auspices of the U.S. Department of Energy by the Lawrence Livermore National Laboratory under Contract No. W7405-ENG-38. R.W.H. acknowledges the support of the U.S. Air Force Office of Scientific Research under Contract No. F49620-88-C-0027 and the National Science Foundation under Grant No. EET-8513857.

¹P. D. Maker and R. W. Terhune, *Phys. Rev.* **137**, A801 (1965).
²M. J. Weber, D. Milam, and W. L. Smith, *Opt. Eng.* **17**, 463 (1978).
³R. W. Hellwarth, *Prog. Quantum Electron.* **5**, 1 (1977).
⁴E. M. Campbell, J. T. Hunt, E. S. Bliss, D. R. Speck, and R. P. Drake, *Rev. Sci. Instrum.* **57**, 2101 (1986).
⁵M. A. Henesian, D. M. Pennington, C. D. Swift, and R. W. Hellwarth, Lawrence Livermore National Laboratory, Livermore, California, 1986 Laser Program Annual Report No. UCRL-50021-86, 1987, pp. 4-71.
⁶M. A. Henesian, R. D. Boyd, J. T. Hunt, D. R. Speck, C. D. Swift, and P. J. Wegner, in *Technical Digest, Conference on Lasers and Electro-Optics, San Francisco, 1986* (Optical So-

ciety of America, Washington, D.C., 1986), paper THA2.
⁷P. D. Maker, R. W. Terhune, and C. M. Savage, *Phys. Rev. Lett.* **12**, 507 (1964).
⁸D. V. Vlasov, R. A. Garaev, V. V. Korobkin, and R. V. Serov, *Zh. Eksp. Teor. Fiz.* **76**, 2039 (1979) [*Sov. Phys.—JETP* **49**, 1033 (1979)].
⁹R. W. Hellwarth, M. A. Henesian, and D. M. Pennington (unpublished).
¹⁰S. Carusotto, E. Iacopini, E. Polacco, F. Scuri, G. Stefanini, and E. Zavattini, *Nuovo Cimento* **5D**, 328 (1985).
¹¹V. Mizrah and D. P. Shelton, *Phys. Rev.* **55**, 696 (1985).
¹²G. C. Herring, M. J. Dyer, and W. K. Bischel, *Opt. Lett.* **11**, 348 (1986).